

Targeting *PPM1D* by lentivirus-mediated RNA interference inhibits the tumorigenicity of bladder cancer cells

W. Wang^{1,3}, H. Zhu³, H. Zhang², L. Zhang², Q. Ding^{1,2} and H. Jiang^{1,2}

¹Institute of Urology, Huashan Hospital, Fudan University, Shanghai, China

²Department of Urology, Huashan Hospital, Fudan University, Shanghai, China

³Department of the Intensive Care Unit, Huashan Hospital, Fudan University, Shanghai, China

Abstract

Protein phosphatase magnesium/manganese-dependent 1D (*PPM1D*) is a p53-induced phosphatase that functions as a negative regulator of stress response pathways and has oncogenic properties. However, the functional role of *PPM1D* in bladder cancer (BC) remains largely unknown. In the present study, lentivirus vectors carrying small hairpin RNA (shRNA) targeting *PPM1D* were used to explore the effects of *PPM1D* knockdown on BC cell proliferation and tumorigenesis. shRNA-mediated knockdown of *PPM1D* significantly inhibited cell growth and colony forming ability in the BC cell lines 5637 and T24. Flow cytometric analysis showed that *PPM1D* silencing increased the proportion of cells in the G0/G1 phase. Downregulation of *PPM1D* also inhibited 5637 cell tumorigenicity in nude mice. The results of the present study suggest that *PPM1D* plays a potentially important role in BC tumorigenicity, and lentivirus-mediated delivery of shRNA against *PPM1D* might be a promising therapeutic strategy for the treatment of BC.

Key words: Protein phosphatase magnesium/manganese-dependent 1D; Bladder cancer; Gene silencing; RNA interference; Proliferation

Introduction

In 2012, bladder cancer (BC) was the fourth most common cancer in males and the eighth most common in females in the United States (1). Approximately 20% of tumor node metastasis (TNM) stage T1 primary tumors that undergo re-resection progress to invasive BC (2,3). In addition, overexpression of p53, p21, and p16 is associated with increased risk of recurrence and poor long-term survival in BC, suggesting that targeted treatment in the early stages of the disease could be a useful strategy (4,5).

Protein phosphatase magnesium/manganese-dependent 1D (*PPM1D*), also called wild-type p53-induced phosphatase (*Wip1*), is a member of the magnesium-dependent serine/threonine protein phosphatase (PPM) family (6,7). It was first identified as a phosphatase induced by p53 in response to ultraviolet and ionizing radiation (8). The *PPM1D* gene is located on chromosome 17q23.2 and is a negative regulator of stress response pathways. *PPM1D* plays a variety of roles in cellular processes, including abrogation of cell cycle checkpoints and inhibition of senescence, apoptosis, and DNA repair (9). Studies have shown that *PPM1D*

possesses oncogenic properties (10,11). Amplified levels of the *PPM1D* gene have been found in several cancer cell lines including neuroblastoma and lung, breast, pancreatic, bladder, and liver cancers (11,12). Moreover, *PPM1D* is overexpressed in a number of human primary tumors, such as breast cancer (13), ovarian cancer (14,15), neuroblastoma (16), hepatocellular cancer (17) and lung cancer (18), and is associated with poor prognosis.

RNA interference (RNAi) is an endogenous protein suppression mechanism by which short double-stranded RNA (dsRNA) mediates sequence-specific degradation of mRNA, thereby preventing translation of the protein encoded by the target mRNA (19,20). RNAi can be used to specifically target mutant genes, cancer-associated genes or receptors involved in oncogenic pathways, thereby opening new avenues in anticancer therapy (21,22). RNAi has been successfully used to control cell proliferation and the invasive ability of BC cells (23).

To elucidate the role of *PPM1D* in BC, we used lentivirus-delivered shRNA to knock down *PPM1D* expression. This

model system was used to examine the effect of *PPM1D* silencing on BC cell proliferation and growth and the antitumor potential of *PPM1D* shRNA *in vivo* and *in vitro*.

Material and Methods

Cells lines and cell culture

The human urinary BC cell lines 5637 and T24 and the human renal epithelial cell line HEK293T were purchased from the American Type Culture Collection (USA) and maintained at 37°C and 5% CO₂. The HEK293T and T24 cell lines were cultured in Dulbecco's modified Eagle's medium (DMEM; Invitrogen, USA) supplemented with 10% fetal bovine serum (FBS, Invitrogen), and the 5637 cell line was cultured in RPMI-1640 (Invitrogen) supplemented with 10% FBS.

Lentiviral plasmid construction, lentivirus production, and cell infection

The human *PPM1D* (Gen-Bank accession no. NM_003620.3) specific small interfering RNA (siRNA) sequence, which was designed with online software from Invitrogen, was 5'-CCCTTCTCGTGGTTTGCTTAAA-3'. The nonsilencing (NS) sequence (5'-TTCTCCGAACGTGTCACGT-3') was used as a scrambled control (24). Pairs of complementary oligonucleotides with these sequences were synthesized, annealed, and ligated into a linearized pGCSIL-GFP plasmid vector. These plasmids were amplified in *E. coli* DH5 and purified using a QIAGEN Plasmid Maxi Kit (Qiagen, The Netherlands). Lentivirus was generated in 293T cells by cotransfection of the recombinant pGCSIL-GFP vector, together with pHelper 1.0 and pHelper 2.0 plasmids using Lipofectamine 2000 (Invitrogen). The lentiviral particles were harvested 48 h after transfection and purified by ultracentrifugation (2 h at 50,000 g) (25), and are hereafter referred to as Lv-si-*PPM1D* (a specific interference construct for *PPM1D*) or Lv-si-CTRL (negative control). For cell infection, 30% confluent 5637 and T24 cells were incubated with lentiviruses for 48 h, and the medium, which contained puromycin (10 µg/mL; Sigma-Aldrich, USA), was replaced to select stable clones. Each cell line was divided into two experimental groups, the si-CTRL group (cells infected with Lv-si-CTRL) and the si-*PPM1D* group (cells infected with Lv-si-*PPM1D*).

Quantitative real-time polymerase chain reaction (PCR) and Western blotting

Total RNA was extracted and reverse-transcribed as described previously (26). Quantitative real-time PCR reactions were carried out with an ABI Prism 7900 Sequence Detection System (PE Applied Biosystems, USA) using 25 µL of a reaction mixture that consisted of 0.1 µM primers, 10 µL 2 × SYBR Premix Ex Taq (Takara, Japan), and 20-100 ng cDNA sample. The following primers were used: *PPM1D*, 5'-AGAGAATGTCCAAGGTGTAGTC

-3' and 5'-TCGTCTATGCTTCTTCATCAGG-3'; β-actin, 5'-GTGGACATCCGCAAAGAC-3' and 5'-TCGTCTATGCTTCTTCATCAGG-3'. An initial denaturation/activation step (15 s, 95°C) was followed by 45 cycles (5 s at 95°C, 30 s at 60°C). The relative expression of *PPM1D* mRNA was calculated with the 2^{-ΔΔCt} method, and β-actin mRNA expression was used for normalization.

Western blot analysis was performed to detect *PPM1D* protein expression. Cells were scraped and homogenized in radioimmunoprecipitation assay (RIPA) lysis buffer. Proteins extracted from cellular lysates were separated on 12% sodium dodecyl (SDS)-polyacrylamide gels and transferred onto polyvinylidene fluoride (PVDF) membranes (Millipore, USA). After blocking, the membranes were incubated with mouse anti-*PPM1D* and anti-*GAPDH* monoclonal antibodies (1:200 and 1:5000, respectively, Santa Cruz Biotechnology, USA) overnight at 4°C. After washing with Tris-buffered saline/Tween-20 solution, the membranes were incubated with horseradish peroxidase-conjugated goat anti-mouse IgG (1:5000, Santa Cruz Biotechnology) at room temperature for 1 h. Bands were detected using an enhanced chemiluminescence system (Amersham, USA).

Cell proliferation and colony formation assay

Cells were trypsinized, resuspended, seeded onto 96-well plates in 100 µL (5 × 10³ cells) per well, and incubated at 37°C. The number of viable cells was measured daily using 3-(4,5-dimethylthiazol-2-yl)-2,5-diphenyltetrazolium bromide (MTT) as described previously (26). For the cell colony formation assay, cells were seeded onto 6-well plates at a density of 200 cells per well and cultured at 37°C for 14 days. After fixing with paraformaldehyde, cells were stained with Giemsa (Sigma) for 10 min, and washed with double distilled H₂O three times. The plates were photographed with a digital camera. Each experiment was performed in triplicate and repeated three times.

Flow cytometric assay

Cells were harvested and fixed with cold 70% ethanol for 1 h. The cells were sequentially centrifuged (5 min at 100 g) and resuspended with phosphate-buffered saline (PBS). Cells were stained with propidium iodide (Sigma-Aldrich) at 4°C for 30 min in the dark and analyzed using flow cytometry. Each experiment was conducted in triplicate.

Animal experiments

Five-week-old male BALB/c mice were purchased from Shanghai Slac Laboratory Animal Co. Ltd. (China) and received humane care in compliance with the Guidelines for the Care and Use of Experimental Animals in Research. Mice were divided into 2 groups of 10 mice each, referred to as the si-CTRL and si-*PPM1D* groups. A total of 5 × 10⁶ Lv-si-CTRL or Lv-si-*PPM1D* infected cells were suspended in Eagle's minimal essential medium (EMEM) and injected subcutaneously into the right flank of each mouse in the

corresponding group. The tumor diameter was measured, and the volume was calculated using the formula $V = 0.4 \times ab^2$ (V = volume, a = largest diameter, b = smallest diameter) on days 10, 14, 18, and 24. Mice were photographed and humanely killed on day 24, and the tumors were dissected and weighed.

Statistical analysis

All data are reported as means \pm SE. Statistical analysis was performed using the Student two-tailed unpaired *t*-test for comparisons between two groups. In all cases, $P < 0.05$ was considered to be statistically significant.

Results

Lentivirus-mediated shRNA inhibited the expression of PPM1D in BC cells

The 5637 and T24 cell lines were infected with Lv-si-*PPM1D*; the highest infection efficiency was $>90\%$, as determined by detecting the expression of green fluorescent protein (GFP) 96 h after infection (Figure 1A). Quantitative real-time PCR analysis showed that the *PPM1D* mRNA level was significantly lower in the si-*PPM1D* group compared to the si-CTRL group (Figure 1B). The protein level of *PPM1D* in the si-*PPM1D* group was also strongly decreased compared with the si-CTRL group (Figure 1C).

Knockdown of PPM1D inhibited BC cell growth

To examine the effect of *PPM1D* knockdown on BC cell

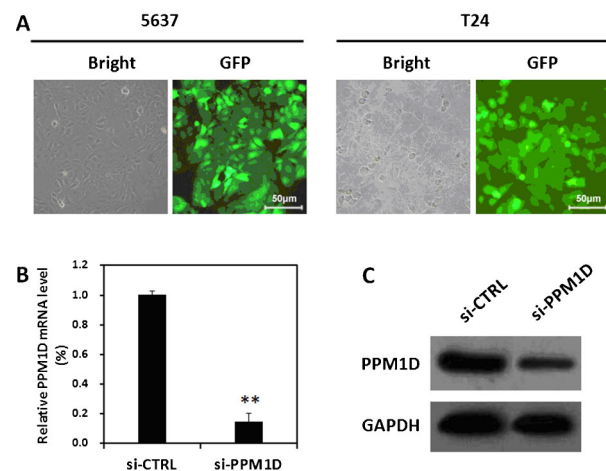


Figure 1. Knockdown of *PPM1D* in bladder cancer cells by lentivirus-mediated shRNA. **A**, Detection of lentiviral infection efficiency. The 5637 and T24 cells were infected with Lv-si-*PPM1D*, and phase contrast (left) or GFP (right) images were obtained 96 h after infection. Magnification: $200\times$. **B**, Analyses of *PPM1D* mRNA expression in 5637 cells by quantitative real-time PCR. **C**, Western blot analysis of *PPM1D* protein expression in 5637 cells. Data are reported as means \pm SD of three independent experiments. ** $P < 0.01$, *t*-test.

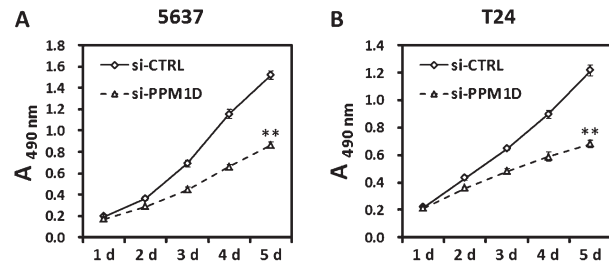


Figure 2. Knockdown of *PPM1D* attenuated the growth potential of bladder cancer cells *in vitro*. The proliferation of 5637 (**A**) and T24 (**B**) cells was assessed by MTT assay after infection with Lv-si-CTRL or Lv-si-*PPM1D*. Data are reported as means \pm SD of three independent experiments. Lv: lentiviral; d: day. ** $P < 0.01$, compared to Lv-si-CTRL (*t*-test).

growth, Lv-si-*PPM1D*- or Lv-si-CTRL-infected 5637 and T24 cells were subjected to MTT and colony formation assays. As shown in Figure 2, cell proliferation in the si-*PPM1D* group was significantly inhibited compared with that in the si-CTRL group. Colony formation ability was significantly lower in the si-*PPM1D* group compared to the si-CTRL group (Figure 3). Similar results were obtained in 5637 and T24 cells.

Flow cytometric analysis showed that the proportion of cells in the G1 phase was markedly increased in the si-*PPM1D* group compared with the si-CTRL group (Figure 4), partly explaining the growth suppression mediated by Lv-si-*PPM1D*.

Knockdown of PPM1D inhibited BC tumorigenicity *in vivo*

The 5637 cells infected with Lv-si-CTRL or Lv-si-*PPM1D* were subcutaneously implanted into nude mice to examine

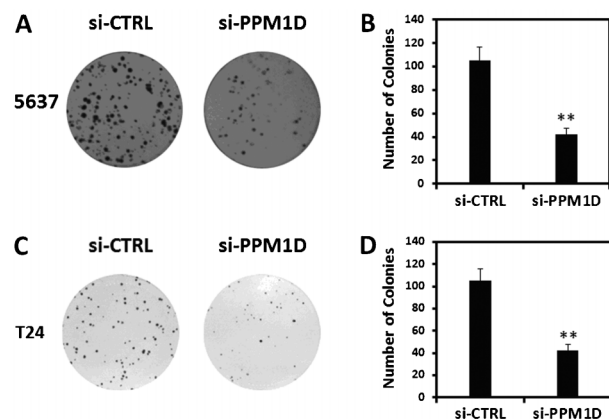


Figure 3. *PPM1D* knockdown decreased the colony formation ability of 5637 (**A,B**) and T24 (**C,D**) cells. Data are reported as means \pm SD of three independent experiments. The number of colonies was significantly different between cells infected with Lv-si-CTRL and with Lv-si-*PPM1D* (** $P < 0.01$, *t*-test).

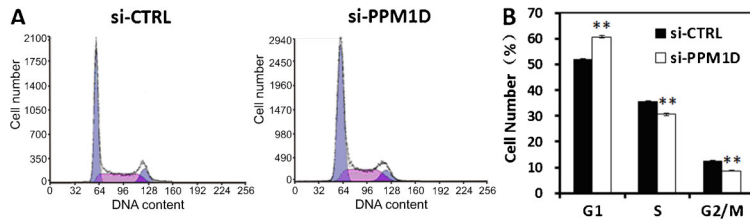


Figure 4. Knockdown of *PPM1D* increases the proportion of 5637 cells in G1 phase. Cell cycle distribution was analyzed by flow cytometry. *A*, Representative images of three independent FACS analyses are shown. *B*, Proportion of cells in the different cell cycle phases. Data are reported as means \pm SD of three independent experiments. ** $P < 0.01$, compared to si-CTRL (*t*-test).

the effect of *PPM1D* knockdown on BC tumorigenicity *in vivo*. All of the mice in the si-CTRL group displayed steadily and progressively growing tumors, whereas the BC cells in the si-*PPM1D* group showed weaker tumorigenicity, and the mice developed smaller tumors (Figure 5).

Discussion

Gene dysregulation is frequently observed in cancer, and gene expression profiles vary among different cancers. *PPM1D* or Wip1 is a serine/threonine phosphatase that is overexpressed and shows oncogenic activity in multiple human cancers (10). However, the role of the *PPM1D* gene in BC has not been investigated to date. To elucidate the function of *PPM1D* in BC, we used lentivirus-mediated RNAi to inhibit *PPM1D* expression in T24 and 5637 cells and investigated the effects of *PPM1D* knockdown in these BC cell lines. A lentiviral vector carrying *PPM1D* shRNA and a GFP reporter gene was constructed, which showed high infection efficiency in 5637 and T24 cells and effectively silenced *PPM1D* expression. These results indicated the successful construction of an effective shRNA vector targeting the *PPM1D* gene.

Lentivirus-mediated *PPM1D* silencing strongly inhibited the growth and proliferation of T24 and 5637 BC cells *in vitro*, as demonstrated by MTT and colony formation

assays. The data showed that the role of *PPM1D* in BC was consistent with that in other cancers (16,27-29). Flow cytometric cell cycle analysis showed that *PPM1D* knockdown increased the proportion of T24 and 5637 BC cells in the G0/G1 phase, indicating that *PPM1D* downregulation blocked cell cycle progression. This could be a mechanism by which *PPM1D* silencing suppresses proliferation.

To determine the therapeutic value of lentivirus-mediated RNAi of *PPM1D* for BC treatment, we analyzed its effect in a xenograft model. The results showed that sh-*PPM1D* lentivirus inhibited 5637 BC cell proliferation and suppressed their tumorigenic potential, indicating that targeting *PPM1D* may be a potential therapeutic strategy for the treatment of BC.

Previous studies have shown that *PPM1D* promotes tumorigenesis in a p53-dependent manner. *PPM1D* is induced by p53 in response to various environmental stresses and facilitates the return of cells to the pre-stress state (6). In addition, *PPM1D* inhibits p53 activity by directly dephosphorylating p53 or its regulators such as *ATM*, *Chk1*, and *Chk2*, which indirectly inhibit p53 activity (10,30). However, T24 and 5637 BC cells have p53 mutations, which implies that *PPM1D* may function in a p53-independent manner in BC cells. *PPM1D* is a target of p53 and other transcription factors, including the estrogen receptor- α and nuclear factor- κ B (NF- κ B) (9). The p38

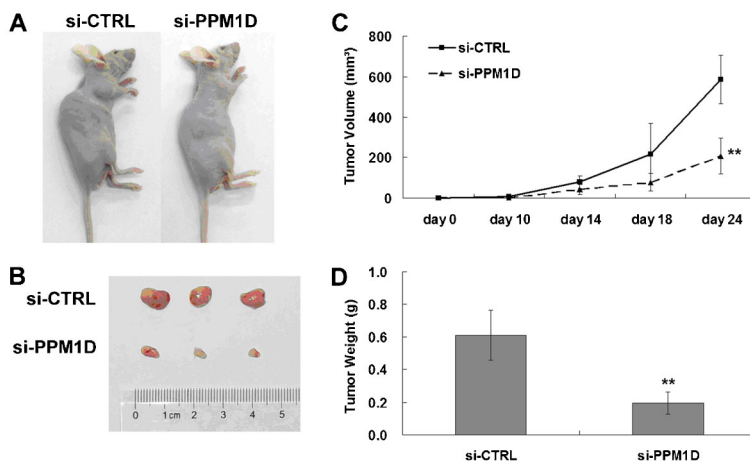


Figure 5. Knockdown of *PPM1D* inhibited the tumorigenicity of bladder cancer cells *in vivo*. Representative photographs of nude mice (*A*) and tumors (*B*) dissected from nude mice 24 days after injection of lentivirus-infected 5637 cells. *C*, Tumor volumes were recorded on days 10, 14, 18, and 24. *D*, Mice were humanely killed and tumors were weighed on day 24. ** $P < 0.01$, compared to si-CTRL (*t*-test).

mitogen-activated protein kinase (MAPK) (31) and Akt (28) signaling pathways may be downstream mediators of *PPM1D* activity in BC. Further studies are required to distinguish these mechanisms.

In conclusion, the results of the present study provided evidence that *PPM1D* plays a potentially important role in BC tumorigenicity and could be a promising target for therapeutic intervention.

References

1. Siegel R, Naishadham D, Jemal A. Cancer statistics, 2013. *CA Cancer J Clin* 2013; 63: 11-30, doi: 10.3322/caac.21166.
2. Vianello A, Costantini E, Del Zingaro M, Bini V, Herr HW, Porena M. Repeated white light transurethral resection of the bladder in nonmuscle-invasive urothelial bladder cancers: systematic review and meta-analysis. *J Endourol* 2011; 25: 1703-1712, doi: 10.1089/end.2011.0081.
3. Ku JH, Lerner SP. Strategies to prevent progression of high-risk bladder cancer at initial diagnosis. *Curr Opin Urol* 2012; 22: 405-414, doi: 10.1097/MOU.0b013e328356adff.
4. Vishnu P, Mathew J, Tan WW. Current therapeutic strategies for invasive and metastatic bladder cancer. *Onco Targets Ther* 2011; 4: 97-113.
5. Gakis G, Schwentner C, Todenhofer T, Stenzl A. Current status of molecular markers for prognostication and outcome in invasive bladder cancer. *BJU Int* 2012; 110: 233-237, doi: 10.1111/j.1464-410X.2011.10839.x.
6. Rossi M, Demidov ON, Anderson CW, Appella E, Mazur SJ. Induction of *PPM1D* following DNA-damaging treatments through a conserved p53 response element coincides with a shift in the use of transcription initiation sites. *Nucleic Acids Res* 2008; 36: 7168-7180, doi: 10.1093/nar/gkn888.
7. Douarre C, Mergui X, Sidibe A, Gomez D, Alberti P, Mailliet P, et al. DNA damage signaling induced by the G-quadruplex ligand 12459 is modulated by *PPM1D*/WIP1 phosphatase. *Nucleic Acids Res* 2013; 41: 3588-3599, doi: 10.1093/nar/gkt073.
8. Fiscella M, Zhang H, Fan S, Sakaguchi K, Shen S, Mercer WE, et al. Wip1, a novel human protein phosphatase that is induced in response to ionizing radiation in a p53-dependent manner. *Proc Natl Acad Sci U S A* 1997; 94: 6048-6053, doi: 10.1073/pnas.94.12.6048.
9. Lowe J, Cha H, Lee MO, Mazur SJ, Appella E, Fornace AJ Jr. Regulation of the Wip1 phosphatase and its effects on the stress response. *Front Biosci* 2012; 17: 1480-1498, doi: 10.2741/3999.
10. Lu X, Nguyen TA, Moon SH, Darlington Y, Sommer M, Donehower LA. The type 2C phosphatase Wip1: an oncogenic regulator of tumor suppressor and DNA damage response pathways. *Cancer Metastasis Rev* 2008; 27: 123-135, doi: 10.1007/s10555-008-9127-x.
11. Bulavin DV, Phillips C, Nannenga B, Timofeev O, Donehower LA, Anderson CW, et al. Inactivation of the Wip1 phosphatase inhibits mammary tumorigenesis through p38 MAPK-mediated activation of the p16(Ink4a)-p19(Arf) pathway. *Nat Genet* 2004; 36: 343-350, doi: 10.1038/ng1317.
12. Bulavin DV, Demidov ON, Saito S, Kauraniemi P, Phillips C, Amundson SA, et al. Amplification of *PPM1D* in human tumors abrogates p53 tumor-suppressor activity. *Nat Genet* 2002; 31: 210-215, doi: 10.1038/ng894.
13. Ruark E, Snape K, Humburg P, Loveday C, Bajrami I, Brough R, et al. Mosaic *PPM1D* mutations are associated with predisposition to breast and ovarian cancer. *Nature* 2013; 493: 406-410, doi: 10.1038/nature11725.
14. Tan DS, Lambros MB, Rayter S, Natrajan R, Vatcheva R, Gao Q, et al. *PPM1D* is a potential therapeutic target in ovarian clear cell carcinomas. *Clin Cancer Res* 2009; 15: 2269-2280, doi: 10.1158/1078-0432.CCR-08-2403.
15. Ali AY, Abedini MR, Tsang BK. The oncogenic phosphatase *PPM1D* confers cisplatin resistance in ovarian carcinoma cells by attenuating checkpoint kinase 1 and p53 activation. *Oncogene* 2012; 31: 2175-2186, doi: 10.1038/ncr.2011.399.
16. Saito-Ohara F, Imoto I, Inoue J, Hosoi H, Nakagawara A, Sugimoto T, et al. *PPM1D* is a potential target for 17q gain in neuroblastoma. *Cancer Res* 2003; 63: 1876-1883.
17. Li GB, Zhang XL, Yuan L, Jiao QQ, Liu DJ, Liu J. Protein phosphatase magnesium-dependent 1 delta (*PPM1D*) mRNA expression is a prognosis marker for hepatocellular carcinoma. *PLoS One* 2013; 8: e60775, doi: 10.1371/journal.pone.0060775.
18. Satoh N, Maniwa Y, Bermudez VP, Nishimura K, Nishio W, Yoshimura M, et al. Oncogenic phosphatase Wip1 is a novel prognostic marker for lung adenocarcinoma patient survival. *Cancer Sci* 2011; 102: 1101-1106, doi: 10.1111/j.1349-7006.2011.01898.x.
19. Castanotto D, Rossi JJ. The promises and pitfalls of RNA-interference-based therapeutics. *Nature* 2009; 457: 426-433, doi: 10.1038/nature07758.
20. Mohr SE, Perrimon N. RNAi screening: new approaches, understandings, and organisms. *Wiley Interdiscip Rev RNA* 2012; 3: 145-158, doi: 10.1002/wrna.110.
21. Bora RS, Gupta D, Mukkur TK, Saini KS. RNA interference therapeutics for cancer: challenges and opportunities (review). *Mol Med Rep* 2012; 6: 9-15.
22. Seth S, Johns R, Templin MV. Delivery and biodistribution of siRNA for cancer therapy: challenges and future prospects. *Ther Deliv* 2012; 3: 245-261, doi: 10.4155/tde.11.155.
23. Zhang H, Jiang H, Wang W, Gong J, Zhang L, Chen Z, et al. Expression of Med19 in bladder cancer tissues and its role on bladder cancer cell growth. *Urol Oncol* 2012; 30: 920-927, doi: 10.1016/j.urolonc.2010.10.003.
24. Pullmann R Jr, Juhaszova M, Lopez dS, I, Kawai T, Mazan-Mamczarz K, Halushka MK, et al. Enhanced proliferation of cultured human vascular smooth muscle cells linked to increased function of RNA-binding protein HuR. *J Biol Chem* 2005; 280: 22819-22826, doi: 10.1074/jbc.M501106200.
25. Sakoda T, Kasahara N, Hamamori Y, Kedes L. A high-titer lentiviral production system mediates efficient transduction

Acknowledgments

This research was supported by grants from the National Natural Science Foundation of China (Project No. 81272835), the Shanghai Science and Technology Commission and international cooperation projects (Project No. 11410708200), and the Shanghai Natural Science Foundation (Project No. 13ZR1405600).

- of differentiated cells including beating cardiac myocytes. *J Mol Cell Cardiol* 1999; 31: 2037-2047, doi: 10.1006/jmcc.1999.1035.
26. Zhang H, Jiang H, Wang W, Gong J, Zhang L, Chen Z, et al. Expression of Med19 in bladder cancer tissues and its role on bladder cancer cell growth. *Urol Oncol* 2012; 30: 920-927, doi: 10.1016/j.urolonc.2010.10.003.
27. Zhang X, Wan G, Mlotshwa S, Vance V, Berger FG, Chen H, et al. Oncogenic Wip1 phosphatase is inhibited by miR-16 in the DNA damage signaling pathway. *Cancer Res* 2010; 70: 7176-7186, doi: 10.1158/0008-5472.CAN-10-0697.
28. Yin H, Yan Z, Liang Y, Liu B, Su Q. Knockdown of protein phosphatase magnesium-dependent 1 (*PPM1D*) through lentivirus-mediated RNA silencing inhibits colorectal carcinoma cell proliferation. *Technol Cancer Res Treat* 2013; 12: 537-543.
29. Parssinen J, Alarmo EL, Karhu R, Kallioniemi A. *PPM1D* silencing by RNA interference inhibits proliferation and induces apoptosis in breast cancer cell lines with wild-type p53. *Cancer Genet Cytogenet* 2008; 182: 33-39, doi: 10.1016/j.cancergencyto.2007.12.013.
30. Zhu YH, Bulavin DV. Wip1-dependent signaling pathways in health and diseases. *Prog Mol Biol Transl Sci* 2012; 106: 307-325, doi: 10.1016/B978-0-12-396456-4.00001-8.
31. Demidov ON, Kek C, Shreeram S, Timofeev O, Fornace AJ, Appella E, et al. The role of the MKK6/p38 MAPK pathway in Wip1-dependent regulation of ErbB2-driven mammary gland tumorigenesis. *Oncogene* 2007; 26: 2502-2506, doi: 10.1038/sj.onc.1210032.